Relationships between nonmesonic weak decays in different hypernuclei

Franjo Krmpotić
Instituto de Física La Plata, Universidad Nacional de La Plata, CONICET, 1900 La Plata, Argentina
(Received 21 June 2009; revised manuscript received 25 May 2010; published 11 November 2010)

Using as a tool the s-wave approximation (sWA), this work demonstrates that the nonmesonic weak decay transition rates Γ_n and Γ_p can be expressed in all hypernuclei up to ${}^{29}_{\Lambda}$Si (and very likely in heavier ones too) in the same way as in the s-shell hypernuclei, i.e., as a linear combination of only three elementary transition rates. This finding leads to the analytic prediction that, independently of the transition mechanism, all hypernuclei that are on the stability line ($\mathsf{N}=\mathsf{Z}$), i.e., ${}^{5}_{\Lambda}$He, ${}^{7}_{\Lambda}$Li, ${}^{9}_{\Lambda}$Be, ${}^{11}_{\Lambda}$B, ${}^{13}_{\Lambda}$C, ${}^{17}_{\Lambda}$O, ${}^{29}_{\Lambda}$Si, etc., should roughly have the same ratio Γ_n/Γ_p, the magnitude of which rapidly increases when one approaches the neutron drip line ($\mathsf{N}\gg\mathsf{Z}$), and the opposite happens when one goes toward the proton drip line ($\mathsf{N}\ll\mathsf{Z}$).

DOI: 10.1103/PhysRevC.82.055204   PACS number(s): 21.80.+a, 13.75.Ev, 21.60.Cs

I. INTRODUCTION

The nonmesonic weak decay (NMWD) of Λ hypernuclei, $\Lambda N\rightarrow nN$, takes place only within a nuclear environment with the decay rate Γ_N $(N=p,n)$. Without producing any additional on-shell particle (as does the mesonic weak decay $\Lambda\rightarrow\pi N$), the mass is changed by 176 MeV, and the strangeness by $|\Delta\mathsf{S}|=1$, which implies the most radical modification of an elementary particle within the nucleus. At the same time, it offers the best opportunity to study the strangeness-changing interaction between hadrons and is the main decay channel for medium and heavy hypernuclei.

With the incorporation of strangeness, the radioactivity domain is extended to three dimensions ($\mathsf{N},\mathsf{Z},\mathsf{S}$), which, because of the additional binding due to the Λ hyperon, is even richer in elements than the ordinary (N,Z) domain. (For instance, while the one-neutron separation energy in ^{20}C is 1.01 MeV, it is 1.63 MeV in ${}^{21}_{\Lambda}$C [1].) This attribute of hypernuclei has motivated a recent proposal to produce neutron-rich Λ hypernuclei at the Japan Proton Accelerator Research Complex (J-PARC), including ${}^{9}_{\Lambda}$He [2].[1]

Important experimental efforts have been invested in hypernuclear weak physics during the last few years [5–16]. The correlative theoretical advances in our knowledge of the NMWD have been also quite significant [17–49]. For recent review articles, see Refs. [50–53]. The ratio $\Gamma_{n/p}\equiv\Gamma_n/\Gamma_p$, together with the asymmetry parameter ratio a_Λ for emission of protons from polarized hypernuclei [37,53], has been in the past and still is the main concern in the physics of NMWD. For a long time, the large experimental value for the $\Gamma_{n/p}$ ratio (close to unity) remained unexplained. But, recent improved data tend to converge to $\cong$0.5 [7–10], both for ${}^{5}_{\Lambda}$He (s shell) and ${}^{12}_{\Lambda}$C (p shell), indicating similarity in the transition mechanism.

In the meantime, the theoretical estimates of $\Gamma_{n/p}$, done within the one meson-exchange (OME) model, have increased. For instance, Parreño and Ramos [24] have found $\Gamma_{n/p}({}^{5}_{\Lambda}\text{He})=0.34$–$0.46$, and $\Gamma_{n/p}({}^{12}_{\Lambda}\text{C})=0.29$–$0.34$, when the exchanges of the complete pseudoscalar (π,K,η) and vector (ρ,ω,K^*) meson octets are taken into account, with the weak coupling constants obtained from soft meson theorems and SU(6)$_W$ [17,18]. The dominant role is played by the exchange of pion and kaon mesons, and when their effect is combined with the direct-quark (DQ) model, the value of the n/p ratio is increased up to 0.70 [20,23]. However, these transition mechanisms continue to predict too large and negative value for a_Λ. There are two recent proposals to bring this value into agreement with experiments by going beyond the OME + DQ models. The first considers incorporating new scalar-isoscalar terms induced by 2π exchanges [38]. (See also Refs. [22,31] on the relevance of these terms.) In the second, in addition to the model of $\pi+2\pi/\rho+2\pi/\sigma+2p/s+\omega+K$ exchanges, is introduced the axial-vector a_1-meson exchange [40].

Quite recently we have discussed the parameter a_Λ within the independent particle shell model (IPSM), together with the s-wave approximation (sWA) [37]. The corollary of this study was that, independently of the NMWD dynamics, this observable has the same value in all hypernuclei that have totally full proton subshells, such as ${}^{5}_{\Lambda}$He and ${}^{12}_{\Lambda}$C, and very likely also in the remaining hypernuclei. This result is a direct consequence of the fact that a_Λ, same as $\Gamma_{n/p}$, is a ratio of two transition rates, which makes it, in the absence of final state interactions (FSI), dependent purely on the dynamical features of the NMWD.

The aim of this work is twofold. First, we establish the link between the theoretical formalism for the NMWD of the s-shell hypernuclei originally introduced by Block and Dalitz [54] and the general formalism used presently for any type of hypernuclei. Second, we show that the IPSM framework, together with the sWA, allows us to formulate the rates Γ_N within the p,d, etc., shells in terms of the s-shell nuclear matrix elements (NME). Previous research in this direction has been done by Alberico and Garbarino [21] and by Cohen [55].

Later on, it is demonstrated that regardless of the decay mechanism, (i) all hypernuclei with the same number of protons and neutrons (i.e., with $\mathsf{Z}=\mathsf{N}$) should have the same ratio $\Gamma_{n/p}$, (ii) the value of this observable increases (decreases) as the neutron (proton) excess is enlarged, and

[1] It is also speculated that the NMWD could have an important role in the stability of rotating neutron stars with respect to gravitational wave emission [3,4].

    ©2010 The American Physical Society

(iii) simple analytic relationships exist between Γ_n, Γ_p, and $\Gamma_{n/p}$ in different hypernuclei with the same mass number A. The derivation of these results, same as those on the parameter a_Λ [37], is based on the assumption that the emission of the nucleons N from different single-particle states is affected in a similar way by the FSI. Then, before presenting the formalism, it might be convenient to comment on the relationship between the ratio Γ_n/Γ_p and the FSI.

The primary partial decay rates Γ_N are in principle derivable from the measurements of emitted nucleons n and N spectra. These are (i) the single-nucleon spectra $S(E_N)$, as a function of one-nucleon kinetic energies E_N, and (ii) nN coincidence spectra $S(E_{nN})$, and $S(\cos\theta_{nN})$, as functions of the sum of kinetic energies $E_{nN} = E_n + E_N$, and the opening angle θ_{nN}, respectively. From these spectra are determined the number of protons N_p and neutrons N_n, and number of pairs N_{nn} and N_{np}, which are not related in a simple way with Γ_n and Γ_p. This is because not all primary nucleons originated by the NMWD are measured. In propagating within the nuclear environment, they interact with the surrounding nucleons, and in some cases they change their momenta and energies, some of them even can be absorbed by the medium, and emission of additional (secondary) nucleons can take place as well [43–48]. All these processes represent a complicated many-body problem and are generically designated as FSI. To describe them, while keeping the calculations feasible, are indispensable model assumptions, and the FSI are usually simulated by a semi-classical model, developed by Ramos *et al.* [19], and called the intranuclear cascade (INC) model. This model interrelates the rates Γ_n and Γ_p with the numbers N_n, N_p, N_{nn}, and N_{np}, and therefore, as stressed recently by Bauer and Garbarino [47], the FSI described by the INC model should not be included in the evaluation of decay rates Γ_n and Γ_p. However, not all FSI are considered within the INC model, and which additional FSI contribute to the NMWD spectra and decay rates, and how and which of them should be included in the calculation are nontrivial questions. Some candidates are as follows:

(i) Short-range correlations (SRCs) acting on final nN states; here one starts from the plane-wave approximation for the outgoing nucleons and the SRCs are incorporated *a posteriori*, either phenomenologically through Jastrow-like SRC functions, or by solving the Bethe-Goldstone equation. The first approach is used within both nuclear matter [30,43–45] and finite nuclei calculations [18,26–28], and the second one only in the shell-model-type calculations [18,24,25,40].

(ii) Self-energy and vertex particle-hole corrections, and RPA-like rescattering effects [see, for instance, diagrams (b)–(d) in Fig. 2 of Ref. [56]]. It is not known whether these FSI contribute coherently or incoherently, and it can even happen that (b) and (c) cancel out, as do the divergences in the vertex, and fermion self-energy corrections in the QED, because of the Ward identity. (Something similar happens also in the nuclear particle-phonon-coupling model.) The first ones can be associated with the mean-field effects on the single-particle wave functions engendered by an energy-dependent complex optical potential [49].

(iii) Interactions of the deep-hole states (which become highly excited states in the continuum after the NMWD) with more complicated configurations (2h1p, 3h2p, ..., collective states, etc.), which spread their transition strengths in relatively large energy intervals [41].

There is no theoretical study in the literature on the NMWD encompassing all aspects of the FSI. The development of a microscopic many-body model for the FSI described by the INC model would be also extremely welcome, and so far only in Refs. [39,45] were the first steps taken toward this goal. Finally, the two-body induced NMWD $\Lambda NN \rightarrow nNN$, which has been recently measured [15], should be also considered.[2] Briefly, the issue of FSI is a tough nut to crack, and a lot of theoretical work has to be done still, particularly in relation to the recently measured spectra $S(E_N)$, $S(E_{nN})$, and $S(\cos\theta_{nN})$ [5–16], which are certainly affected by them. However, as the purpose of the present contribution is not to make progress in this direction, among all possible FSI, only the SRCs will be considered here. This is done phenomenologically, and initial ΛN state SRCs are included on the same footing [18,26–28]. It is our belief that this is a fair approximation for the objectives of the present work.

II. DECAY RATES

To derive the NMWD rate within the IPSM, we start with the Fermi Golden Rule. For a hypernucleus, in its ground state with spin J_I and energy E_{J_I}, decaying to (i) several states α_N in the residual nuclei with spins J_F and energies $E_{\alpha_N J_F}$, and (ii) two free nucleons n and N, with momenta $\mathbf{p}_n$, and $\mathbf{p}_N$, kinetic energies $E_n = \mathbf{p}_n^2/2M$, and $E_N = \mathbf{p}_N^2/2M$, and total spin S, reads [26–28]

$$\Gamma_N = 2\pi \sum_{S\alpha_N J_F} \int \delta\left(\Delta_{\alpha_N J_F} - E_R - E_n - E_N\right) \times |\langle \mathbf{p}_n \mathbf{p}_N S; \alpha_N J_F | V | J_I \rangle|^2 \frac{d\mathbf{p}_n}{(2\pi)^3} \frac{d\mathbf{p}_N}{(2\pi)^3}, \tag{2.1}$$

where for sake of simplicity we have suppressed the magnetic quantum numbers. The NMWD dynamics, contained within the weak hypernuclear transition potential V, will be described by the OME model. The wave functions for the kets $|\mathbf{p}_n \mathbf{p}_N S M_S J_F M_F\rangle$ and $|J_I M_I\rangle$ are assumed to be antisymmetrized and normalized, and the two emitted nucleons n and N are described by plane waves. Initial and final SRCs are included phenomenologically at a Jastrow-like level, while the finite nucleon size effects at the interaction vertices are gauged by monopole form factors [18,26]. Moreover,

$$E_R = \frac{|\mathbf{p}_n + \mathbf{p}_N|^2}{2M(A-2)} = \frac{E_n + E_N + 2\cos\theta_{nN}\sqrt{E_n E_N}}{A-2} \tag{2.2}$$

is the recoil energy of the residual nucleus, and

$$\Delta_{\alpha_N J_F} = \Delta + E_{J_I} - E_{\alpha_N J_F}, \tag{2.3}$$

with $\Delta = M_\Lambda - M = 176$ MeV, is the liberated energy.

[2]It also has been shown that the kinematical and nonlocal and kinematical effects on the NMWD could be sizable [27].

It could be convenient to perform a transformation to the relative and c.m. (i) momenta $\mathbf{p} = (\mathbf{p}_n - \mathbf{p}_N)/2$, $\mathbf{P} = \mathbf{p}_n + \mathbf{p}_N$, (ii) coordinates $\mathbf{r} = \mathbf{r}_n - \mathbf{r}_N$, $\mathbf{R} = (\mathbf{r}_n + \mathbf{r}_N)/2$, and (iii) orbital angular momenta $\mathbf{l}$ and $\mathbf{L}$. The energy conservation is expressed as

$$E_n + E_N + E_R - \Delta_{\alpha_N J_F} = \epsilon_p + \epsilon_P - \Delta_{\alpha_N J_F} = 0, \quad (2.4)$$

where

$$\epsilon_p = \frac{p^2}{M}, \quad E_R = \frac{P^2}{2M(A-2)}, \qquad \epsilon_P = \frac{P^2}{4M}\frac{A}{A-2} = \frac{A}{2}E_R, \quad (2.5)$$

are, respectively, the energies of the relative motion of the outgoing pair, of the recoil, and of the total c.m. motion (including the recoil).

Following the analytical developments done in Ref. [26], the transition rate can be expressed as a function of the c.m. momentum P:

$$\Gamma_N = \frac{2M}{\pi}\sqrt{\frac{A-2}{A}}\int dP \sum_{\alpha_N J_F} P^2 \sqrt{P^2_{\Delta_{\alpha_N J_F}} - P^2}\,\mathcal{F}_{\alpha_N J_F}(pP), \quad (2.6)$$

with

$$\mathcal{F}_{\alpha_N J_F}(pP) = \hat{J}_I^{-2}\sum_{S\lambda l L T J}\left|\sum_{j_N}\mathcal{M}(plPL\lambda SJ\mathsf{T}; j_\Lambda j_N J \mathsf{t}_{\Lambda N}) \times \langle J_I\|\big(a^\dagger_{j_N}a^\dagger_{j_\Lambda}\big)_J\|\alpha_N J_F\rangle\right|^2, \quad (2.7)$$

where

$$P_{\Delta_{\alpha_N J_F}} = 2\sqrt{\frac{A-2}{A}\Delta_{\alpha_N J_F}}, \quad (2.8)$$

and

$$p = \frac{1}{2}\sqrt{\frac{A}{A-2}\left[P^2_{\Delta_{\alpha_N J_F}} - P^2\right]}, \quad (2.9)$$

It is clear that the condition $P \leqslant P_{\Delta_{\alpha_N J_F}}$ has to be fulfilled for each final state $|\alpha_N J_F\rangle$. Moreover,

$$\mathcal{M}(plPL\lambda SJ\mathsf{T}; j_\Lambda j_N J\mathsf{t}_{\Lambda N}) = \frac{1}{\sqrt{2}}[1-(-)^{l+S+T}]\mathcal{O}_L(P)(lL\lambda SJ\mathsf{T}|V(p)|j_\Lambda j_N J\mathsf{t}_{\Lambda N}), \quad (2.10)$$

where (and henceforth) the ket $|)$, unlike $|\rangle$, indicates that the state is not antisymmetrized,

$$\mathcal{O}_L(P) = \int R^2 dR\, j_L(PR)\mathrm{R}_{0L}(b/\sqrt{2}, R), \quad (2.11)$$

is the overlap of the c.m. radial wave functions R_{0L}, and j_L for the bound and outgoing particles, respectively, and b is the harmonic oscillator size parameter. More, $\boldsymbol{\lambda} = \mathbf{l} + \mathbf{L}$, $\mathsf{T} \equiv \{TM_T, M_T = m_{t_\Lambda} + m_{t_N}\}$, and $\mathsf{t}_{\Lambda N} \equiv \{t_\Lambda = 1/2, m_{t_\Lambda} = -1/2, t_N = 1/2, m_{t_N}\}$, with $m_{t_p} = 1/2$, and $m_{t_n} = -1/2$, where we have assumed that the $\Lambda N \to nN$ interaction occurs with the isospin change $\Delta T = 1/2$. Explicitly,

$$|\mathsf{t}_{\Lambda N}) = \begin{cases} |T=1), & \text{for} \quad N = n \\ (|T=1) - |T=0))/\sqrt{2}, & \text{for} \quad N = p \end{cases}. \quad (2.12)$$

It might be pertinent to mention that the factor $(A-2)/A$ in Eqs. (2.6), (2.8), and (2.9) comes from the recoil effect, which, in the same way as the spreading of the deep-hole states, is relevant for the NMWD spectra [41,42], but its role is of minor importance for the total transition rates Γ_N.

A. Independent-particle shell model

Up to now nothing has been said about the initial state $|J_I\rangle$ and final states $|\alpha_N J_F\rangle$. Within the IPSM, the following assumptions are made, which greatly simplify the numerical calculations:

(i) The initial hypernuclear state is taken as a Λ particle in single-particle state $j_\Lambda = 0s_{1/2}$ weakly coupled to an $(A-1)$ nuclear core of spin J_C, i.e., $|J_I\rangle \equiv |(J_C j_\Lambda)J_I\rangle$.

(ii) When the nucleon inducing the decay is the single-particle state j_N ($j \equiv nlj$), the final residual nucleus states are $|\alpha_N J_F\rangle \equiv |(J_C j_N^{-1})J_F\rangle$.

(iii) We adopt the simplest version of the IPSM, in which all the relevant particle states are assumed to be stationary, and the liberated energy is

$$\Delta_N^j = \Delta + \varepsilon_\Lambda + \varepsilon_N^j, \quad (2.13)$$

where $N = p, n$, and ε are single-particle energies. (The nonstationary version of the IPSM is discussed in Ref. [41].)

Within this scheme, we get [26,28]

$$\Gamma_N = \sum_j \Gamma_N^j, \quad \Gamma_N^j = \sum_{J=|j-1/2|}^{J=j+1/2} F^j_{NJ}\mathcal{R}^j_{NJ}, \quad (2.14)$$

where the summation goes over all single-particle transition rates Γ_N^j, which in turn results from the sum over the values of $\boldsymbol{J} = \boldsymbol{j}_N + \boldsymbol{j}_\Lambda$ of products of the spectroscopic factors F^j_{NJ} with the partial $\Lambda n \to nN$ transition rates $\mathcal{R}^j_{NJ}$. For the s-shell nuclei, the latter have the same physical meaning as the quantities R_{NJ} introduced in the seminal work of Block and Dalitz [54] (see also Ref. [55]), i.e., $\mathcal{R}^{s_{1/2}}_{NJ} \equiv R_{NJ}$.[3]

The spectroscopic factors F^j_{NJ} are defined as

$$F^j_{NJ} = \hat{J}_I^{-2}\sum_{J_F}|\langle J_I\|\big(a^\dagger_{j_N}a^\dagger_{j_\Lambda}\big)_J\|J_F\rangle|^2 = \hat{J}^2\sum_{J_F}\begin{Bmatrix} J_C & J_I & j_\Lambda \\ J & j_N & J_F\end{Bmatrix}^2 |\langle J_C\|a^\dagger_{j_N}\|J_F\rangle|^2, \quad (2.15)$$

[3] In order to use here the same notation for R_{NJ} as in Ref. [54], as well as to write $\mathcal{R}^j_{NJ}$ instead of $\mathcal{R}^{j_N}_J$, the j_N variable employed in previous publications is frequently split here into j and N.

with the notation $\hat{J} = \sqrt{2J+1}$, while the partial transition rates read

$$\mathcal{R}^j_{NJ} = \frac{2M_{\rm N}}{\pi}\sqrt{\frac{A}{A-2}}\int_0^{P^j_N} dP\,P^2\sqrt{\left(P^j_N\right)^2 - P^2} \times \sum_{SlL\lambda T} |\mathcal{M}(plPL\lambda SJ\mathsf{T}; j_\Lambda j_N J\mathsf{t}_{\Lambda N})|^2, \quad (2.16)$$

with

$$P^j_N = 2\sqrt{\frac{A-2}{A}M_{\rm N}\Delta^j_N} \quad (2.17)$$

the maximum value of P for each j_N, and

$$p = \frac{1}{2}\sqrt{\frac{A}{A-2}\left[\left(P^j_N\right)^2 - P^2\right]} \quad (2.18)$$

the corresponding relative momentum.

It should be stressed that the most important virtue of the IPSM is that the index α becomes superfluous, and the summation on the final spins J_F can be carried out without knowing the nuclear structure of the initial and final nuclear states. This simplifies enormously the numerical calculations. As far as we know, the IPSM has been used to a great extent in all previous finite nucleus evaluation of the NMWD.

B. *s*-wave approximation

Galeão [57] has shown that the matrix elements in Eq. (2.10) can be cast in the form

$$(lL\lambda SJ\mathsf{T}|V(p)|j_\Lambda j_N J\mathsf{t}_{\Lambda N}) = \sum_{KS'\mathsf{l}}(lSK\mathsf{T}|V(p)|\mathsf{l}S'K\mathsf{t}_{\Lambda N})C_{\mathsf{l}}(lL\lambda SJl_N j_N; KS'), \quad (2.19)$$

with

$$C_{\mathsf{l}}(lL\lambda SJl_N j_N; KS') = (-)^{j_N+\frac{1}{2}+S+\lambda}\hat{l}_N\hat{\lambda}\hat{j}_N\hat{S}'\hat{K}^2(0\mathsf{l}0Ll_N|000l_Nl_N) \times \begin{Bmatrix} J & j_N & \frac{1}{2} \\ \frac{1}{2} & S' & l_N \end{Bmatrix}\begin{Bmatrix} L & l & \lambda \\ S & J & K \end{Bmatrix}\begin{Bmatrix} L & K & J \\ S' & l_N & \mathsf{l} \end{Bmatrix}, \quad (2.20)$$

where $(0\cdots|\cdots l_N)$ are the Moshinsky brackets [58]. The plain sWA implies that we make $\mathsf{l}=0$ in Eqs. (2.19) and (2.20), which leads to

$$(lL\lambda SJ\mathsf{T}|V(p)|j_\Lambda j_N J\mathsf{t}_{\Lambda N}) = \sum_{K=0,1} C_0(l\lambda SJl_N j_N; K)(lSK\mathsf{T}|V(p)|0KK\mathsf{t}_{\Lambda N}), \quad (2.21)$$

with

$$C_0(l\lambda SJl_N j_N; K) = \hat{K}^2\hat{\lambda}\hat{j}_N(000l_Nl_N|000l_Nl_N)\delta_{Ll_N}(-)^{j_N+\frac{1}{2}+S+\lambda+l_N+K+J} \times \begin{Bmatrix} J & j_N & \frac{1}{2} \\ \frac{1}{2} & K & l_N \end{Bmatrix}\begin{Bmatrix} K & l & S \\ \lambda & J & l_N \end{Bmatrix}. \quad (2.22)$$

In particular, for the *s*-shell hypernuclei,

$$C_0(llSJ0, 1/2; K) = \delta_{JK}, \quad (2.23)$$

and using Eqs. (2.10) and (2.12), Eq. (2.16) becomes

$$\mathcal{R}^{s_{1/2}}_{NJ} \equiv R_{NJ} = (1+\delta_{nN})\frac{2M_N}{\pi}\sqrt{\frac{A}{A-2}} \times \int_0^{P_N} dP\,P^2\sqrt{P_N^2 - P^2}\mathcal{O}_0^2(P)\sum_{SlT}[1-(-)^{l+S+T}] \times |(lSJ\mathsf{T}|V(p)|0JJ\mathsf{T})|^2, \quad (2.24)$$

where $P_N \equiv P^{s_{1/2}}_N$, and

$$\mathcal{O}_0^2(P) = \left(\frac{\pi}{2}\right)^{1/2} b^3 e^{-(Pb)^2/2}. \quad (2.25)$$

As is well known, the corresponding transition rates

$$\begin{aligned} &\Gamma_N\left({}^3_\Lambda\mathrm{H}\right) = \tfrac{3}{4}R_{N0} + \tfrac{1}{4}R_{N1}, \\ &\Gamma_n\left({}^4_\Lambda\mathrm{H}\right) = \tfrac{1}{2}R_{n0} + \tfrac{3}{2}R_{n1}, \quad \Gamma_p\left({}^4_\Lambda\mathrm{H}\right) = R_{p0}, \\ &\Gamma_p\left({}^4_\Lambda\mathrm{He}\right) = \tfrac{1}{2}R_{p0} + \tfrac{3}{2}R_{p1}, \quad \Gamma_n\left({}^4_\Lambda\mathrm{He}\right) = R_{n0}, \\ &\Gamma_N\left({}^5_\Lambda\mathrm{He}\right) = \tfrac{1}{2}R_{N0} + \tfrac{3}{2}R_{N1}, \end{aligned} \quad (2.26)$$

with $N = n, p$, depend only on four single-particle transition rates R_{n0}, R_{n1}, R_{p0}, and R_{p1}.

Here we will express the Γ_N of heavier hypernuclei in the same way as was done in Eq. (2.26) for the *s*-shell hypernuclei, i.e., as a linear combination of R_{N0} and R_{N1} only:

$$\Gamma_N = \mathcal{F}_{N0}R_{N0} + \mathcal{F}_{N1}R_{N1}. \quad (2.27)$$

To derive the generalized spectroscopic factors (GSFs) $\mathcal{F}_{N0}$ and $\mathcal{F}_{N1}$ for hypernuclei up to ${}^{29}_\Lambda$Si, we perform summations over λ in Eq. (2.16) for each single-particle state $j = p_{3/2}, p_{1/2}$, and $j = d_{5/2}$. The resulting $\mathcal{R}^j_{NJ}$ turn out to be quite similar to Eq. (2.24) for $\mathcal{R}^{s_{1/2}}_{NJ}$, except that now P_N and $\mathcal{O}_0(P)$ are substituted, respectively, by P^j_N and $\mathcal{O}_{l_N}(P)$. Thus, we supplement the plain sWA with the substitutions

$$\begin{aligned} P^j_N &\to P_N, \\ \mathcal{O}_{l_N}(P) &\to \mathcal{O}_0(P), \end{aligned} \quad (2.28)$$

which are fair approximations for the evaluations of ratios Γ_n/Γ_p and a_Λ.[4] In this way we get

$$\begin{aligned} &\mathcal{R}^{p_{3/2}}_{N1} = \frac{R_{N0}}{3} + \frac{R_{N1}}{6}, \quad \mathcal{R}^{p_{3/2}}_{N2} = \frac{R_{N1}}{2}, \\ &\mathcal{R}^{p_{1/2}}_{N1} = \frac{R_{N0}}{6} + \frac{R_{N1}}{3}, \quad \mathcal{R}^{p_{1/2}}_{N0} = \frac{R_{N1}}{2}, \\ &\mathcal{R}^{d_{5/2}}_{N2} = \frac{3R_{N0}}{20} + \frac{R_{N1}}{10}, \quad \mathcal{R}^{d_{5/2}}_{N3} = \frac{R_{N1}}{4}, \end{aligned} \quad (2.29)$$

where the numerical factors come from the summation on λ of the squares of coefficients $C_0(l\lambda SJl_N j_N; K)$ given by Eq. (2.22).

[4] This sWA has been used in Ref. [37] to relate the matrix elements $\mathcal{M}(plPL\lambda SJ\mathsf{T}; j_\Lambda j_N = 0p_{3/2}, J\mathsf{t}_{\Lambda N})$, and $(plSJ\mathsf{T}|V|\mathsf{l}=0, JJ\mathsf{t}_{\Lambda N})$ in ${}^{12}_\Lambda$C [see Eq. (B2) of Ref. [37]]. There are two misprints in Eq. (B2) [37]. The correct results are $\mathcal{M}(p2, P1, 1110; \Lambda\mathrm{p}) = \frac{1}{2\sqrt{6}}\mathsf{d}(p)(P1|11)$, and $\mathcal{M}(p2, P1, 2120; \Lambda\mathrm{p}) = \frac{\sqrt{3}}{2\sqrt{10}}\mathsf{d}(p)(P1|11)$.

It could be useful to express Eq. (2.24) within the Block-Dalitz notation [54]:

$$\begin{aligned} \mathsf{a} &= \langle {}^1S_0|V|{}^1S_0\rangle, \quad \mathsf{b} = \langle {}^3P_0|V|{}^1S_0\rangle, \\ \mathsf{c} &= \langle {}^3S_1|V|{}^3S_1\rangle, \quad \mathsf{d} = \langle {}^3D_1|V|{}^3S_1\rangle, \\ \mathsf{e} &= \langle {}^1P_1|V|{}^3S_1\rangle, \quad \mathsf{f} = \langle {}^3P_1|V|{}^3S_1\rangle, \end{aligned} \tag{2.30}$$

for the NME. Assuming the same value of single-particle energies for protons and neutrons in the state $0s_{1/2}$, one gets the well-known results

$$\begin{aligned} R_{n0} &= 2(a^2+b^2), \quad R_{p0} = a^2+b^2, \\ R_{n1} &= 2f^2, \quad R_{p1} = c^2+d^2+e^2+f^2, \end{aligned} \tag{2.31}$$

where

$$a = \frac{M_{\rm N}}{\pi}\sqrt{\frac{A}{A-2}}\int_0^{P_N} dP\,P^2\sqrt{P_N^2-P^2}\mathcal{O}_0^2(P)\mathsf{a}^2(p), \tag{2.32}$$

and similarly for $b, \ldots, f$. As the NME depends very weakly on the momentum p, we can compute them at $p = p_\Delta \equiv \sqrt{M_{\rm N}\Delta}$ [37], and write

$$a = \mathcal{J}_0\mathsf{a}^2(p_\Delta), \text{ etc.}, \tag{2.33}$$

with

$$\mathcal{J}_0 = \frac{2M_{\rm N}}{\pi}\sqrt{\frac{A}{A-2}}\int_0^{P_N} dP\,P^2\sqrt{P_N^2-P^2}\mathcal{O}_0^2(P), \tag{2.34}$$

which after performing the integration reads [59]

$$\mathcal{J}_0 = 2M_{\rm N}^2\sqrt{2\pi\frac{A-2}{A}}\Delta_N b e^{-z} I_1(z), \tag{2.35}$$

where $I_1(z)$ is a modified Bessel function of the first kind, and

$$z = \Delta_N M_{\rm N} b^2\frac{A-2}{A}. \tag{2.36}$$

Using the asymptotic form of $I_1(z)$ $[I_1(z) \cong e^z/\sqrt{2\pi z}]$, one gets

$$\mathcal{J}_0 = 2\sqrt{M_{\rm N}^3\Delta_N} \simeq 2M_N p_\Delta, \tag{2.37}$$

which is the same result as that derived previously in Ref. [37], where the recoil effect was not considered. Therefore one sees that after performing the integration in Eq. (2.32), this effect is totally washed out from the transition rates.

To evaluate the Γ_N from Eq. (2.14), as well as to derive the GSFs in Eq. (2.27), we need to know the spectroscopic factors F_{NJ}^j given by Eq. (2.15). These, in turn, depend on the angular momenta J_C and J_I, which are fixed from the experimental data and are exhibited in Table I. The F_{NJ}^j values for most of the hypernuclei discussed here are listed in Table I of Ref. [28]. The remaining can be easily inferred from this table, except for the p-wave ones in ${}^7_\Lambda$Li ($F_{N1}^{p_{3/2}} = 5/8$, and $F_{N2}^{p_{3/2}} = 3/8$), and in ${}^9_\Lambda$Be ($F_{N1}^{p_{3/2}} = 3/4$, and $F_{N2}^{p_{3/2}} = 5/4$). The resulting GSFs $\mathcal{F}_{NJ}$ are listed in Table I. It is noticeable that in the jj closed shells the singlet to triplet ratio ($\mathcal{F}_{N0} : \mathcal{F}_{N1}$) is always (1:3).

In all hypernuclei heavier than ${}^5_\Lambda$He, the contribution of the state $0s_{1/2}$ to the total rate Γ_N is

$$\Gamma_N^s = \tfrac{1}{2}R_{N0} + \tfrac{3}{2}R_{N1}, \tag{2.38}$$

TABLE I. Core spins J_C, initial spins J_I, and generalized spectroscopic factors $\mathcal{F}_{NJ}$ within the jj coupling.

${}^A_\Lambda Z$	J_C, J_I	$\mathcal{F}_{n0}$	$\mathcal{F}_{n1}$	$\mathcal{F}_{p0}$	$\mathcal{F}_{p1}$
${}^5_\Lambda$He	$0, \frac{1}{2}$	1/2	3/2	1/2	3/2
${}^7_\Lambda$Li	$1, \frac{1}{2}$	17/24	43/24	17/24	43/24
${}^9_\Lambda$He	$0, \frac{1}{2}$	1	3	1/2	3/2
${}^9_\Lambda$Be	$0, \frac{1}{2}$	5/8	15/8	5/8	15/8
${}^9_\Lambda$C	$0, \frac{1}{2}$	1/2	3/2	1	3
${}^{11}_\Lambda$B	$3, \frac{5}{2}$	25/24	59/24	25/24	59/24
${}^{12}_\Lambda$C	$\frac{3}{2}, 1$	13/12	29/12	1	3
${}^{13}_\Lambda$C	$0, \frac{1}{2}$	1	3	1	3
${}^{21}_\Lambda$C	$0, \frac{1}{2}$	13/8	39/8	1	3
${}^{16}_\Lambda$O	$\frac{1}{2}, 1$	7/6	10/3	5/4	15/4
${}^{17}_\Lambda$O	$0, \frac{1}{2}$	5/4	15/4	5/4	15/4
${}^{28}_\Lambda$Si	$\frac{5}{2}, 2$	33/20	23/5	13/8	39/8
${}^{29}_\Lambda$Si	$0, \frac{1}{2}$	13/8	39/8	13/8	39/8

while the contributions of the single-particle states $0p_{3/2}$, $0p_{1/2}$, etc., depend on their occupations, which, in turn, are reflected in the values of the GSFs listed in Table I. For instance, $\Gamma_p^{p_{3/2}} = \Gamma_p^s$ and $\Gamma_n^{p_{3/2}} = \Gamma_n^s$ in all hypernuclei with $\mathsf{Z} \geqslant 6$ and $\mathsf{N} \geqslant 6$, respectively. In the same way, $\Gamma_p^{p_{1/2}} = \Gamma_p^s/2$ and $\Gamma_n^{p_{1/2}} = \Gamma_n^s/2$ in all hypernuclei with $\mathsf{Z} \geqslant 8$ and $\mathsf{N} \geqslant 8$, respectively. The orbital $0d_{5/2}$ supplies less transition strength than the $0s_{1/2}$ state, and it is given by

$$\Gamma_N^{d_{5/2}} = \tfrac{3}{8}(R_{N0} + 3R_{N1}), \tag{2.39}$$

in all hypernuclei with $\mathsf{Z} \geqslant 14$ or $\mathsf{N} \geqslant 14$.

Several years ago, by means of the sWA, Cohen [55] arrived at the estimate

$$\Gamma_{n/p} = \frac{R_{n0} + 3R_{n1}}{R_{p0} + 3R_{p1}}, \tag{2.40}$$

for the "heavy species" of hypernuclei. From Table I, one sees, however, that this relation is (i) strictly fulfilled only for $\mathsf{N} = \mathsf{Z}$ nuclei, i.e., ${}^5_\Lambda$He, ${}^9_\Lambda$Be, ${}^{13}_\Lambda$C, ${}^{17}_\Lambda$O, and ${}^{29}_\Lambda$Si, (ii) approximately correct for hypernuclei with $\mathsf{N} \cong \mathsf{Z}$, and (iii) totally invalid for hypernuclei far from the stability line.

Moreover, as all hypernuclei with the same A hold the same elementary rates (2.24), very simple relationships can be established from Table I between their rates Γ_p, and Γ_n, and ratios $\Gamma_{n/p}$. For instance,

$$\begin{aligned} \Gamma_p\left({}^9_\Lambda\text{He}\right) &= 0.8\Gamma_p\left({}^9_\Lambda\text{Be}\right) = 0.5\Gamma_p\left({}^9_\Lambda\text{C}\right), \\ \Gamma_n\left({}^9_\Lambda\text{He}\right) &= 1.6\Gamma_n\left({}^9_\Lambda\text{Be}\right) = 2\Gamma_n\left({}^9_\Lambda\text{C}\right), \\ \Gamma_{n/p}\left({}^9_\Lambda\text{He}\right) &= 2\Gamma_{n/p}\left({}^9_\Lambda\text{Be}\right) = 4\Gamma_{n/p}\left({}^9_\Lambda\text{C}\right). \end{aligned} \tag{2.41}$$

These and similar results for other values of A are very likely independent of both the decay mechanism and the final-state interactions.

Detailed calculations of Refs. [18,25,26] have proved that the contribution of the p partial wave to NMWD in p-shell hypernuclei, as well as in heavy-mass systems, is relatively small ($\lesssim$10%). In particular, Itonaga *et al.* [25]

have explored the decay rates Γ_n and Γ_p in hypernuclei from $A = 4$ up to $A = 209$, establishing that the p-wave contributions to the calculated total one-nucleon induced decay rates $\Gamma_{nm} = \Gamma_p + \Gamma_n$ and ratios $\Gamma_{n/p}$ are only a few percent of the respective s-wave contributions (see Fig. 9 of Ref. [25]). They have attributed this finding to the short range of the decay interaction. In fact, it is well known that the ranges of the radial pieces $v(r)$ of the OME potentials are inversely proportional to the meson masses (see Figs. 3–5 in Ref. [25]), the largest inverse mass being that of the pion ($m_\pi^{-1} = 1.4$ fm). Then, when one analyzes the radial matrix element in Eq. (2.19), which reads [see Eq. (A19) of Ref. [27]]

$$(pl|v(r)|0\mathsf{l}) = \int r^2 dr j_l(pr) g_{NN} v(r) g_{N\Lambda} \mathrm{R}_{0\mathsf{l}}(\sqrt{2}b, r), \tag{2.42}$$

where $g_{N\Lambda}$ and g_{NN} are, respectively, the initial and final SRC functions, one can see that (i) the harmonic oscillator wave function $\mathrm{R}_{0\mathsf{l}}(\sqrt{2}b, r)$ is picked at the origin for $\mathsf{l} = 0$, and (ii) the integrand maxima for $\mathsf{l} = 1$, which in principle should be at the distance $\sqrt{2}b$ (= 2.5 fm for $^{12}_{\Lambda}$C) from the origin, is shifted even farther because of the factor r^2. This, together with the approximation (2.28) for the c.m. overlaps, makes the s-wave radial matrix elements large compared to the p-wave ones. Moreover, it could be worth mentioning that with the Wood-Saxon radial wave functions, one gets analogous results since they are quite similar to that of the harmonic oscillator, as can be seen, for instance, from Fig. 2-22 in Ref. [60].

III. COMPARISON BETWEEN EXACT AND sWA RESULTS

For the hypernuclei of interest here, the approximated results are confronted numerically with the full calculations in Table II. This is done within the following framework: (a) The NMWD dynamics is described by the $\pi + K$ OME potential, with the weak coupling constants from Refs. [18,24]. (b) The parameter b is evaluated as in Ref. [28], i.e., $b = 1/\sqrt{\hbar\omega M_{\mathrm{N}}}$, with $\hbar\omega = 45A^{-1/3} - 25A^{-2/3}$ MeV. (c) The initial and final SRC, as well as the finite nucleon size effects, are included in the same way as in our previous works [26–28,37]. The results displayed in Table II clearly show that the agreement between the exact and sWA results is indeed quite satisfactory. In fact, the differences between them are of the same order of magnitude or smaller than that of the kinematical and nonlocality effects discussed in Ref. [27].

A more rigorous inclusion of the strong interaction ingredients on the initial and final two-body states, as done in Refs. [24,25,40], will modify in the same way as the exact and sWA results, without affecting the conclusions of the present work. Namely, there is no physical reason why the mixing between states with the same total angular momenta and different orbital and spin angular momenta—induced by the SRC and exhibited in Eqs. (46) and (47) of Ref. [40]—should influence differently the exact and sWA calculations. That this is true for the final state follows immediately from the fact that the sWA is done only on the initial state. Thus, all the discussion performed in Refs. [24,40] for the final-state tensor correlation is equally valid for both calculations. The initial

TABLE II. Results for exact and sWA transition rates, evaluated, respectively, from Eqs. (2.14) and (2.27). Those for $^{9}_{\Lambda}$Be are not shown, since they fall in between those for $^{9}_{\Lambda}$He and $^{9}_{\Lambda}$C.

$^{A}_{\Lambda}Z$	Approx.	Γ_n	Γ_p	Γ_{nm}	$\Gamma_{n/p}$
$^{5}_{\Lambda}$He	Exact	0.149	0.358	0.507	0.417
$^{7}_{\Lambda}$Li	Exact	0.154	0.375	0.529	0.409
	sWA	0.153	0.369	0.523	0.416
$^{9}_{\Lambda}$He	Exact	0.265	0.317	0.583	0.836
	sWA	0.262	0.318	0.581	0.824
$^{9}_{\Lambda}$C	Exact	0.131	0.676	0.807	0.194
	sWA	0.131	0.637	0.768	0.206
$^{11}_{\Lambda}$B	Exact	0.208	0.528	0.736	0.394
	sWA	0.207	0.499	0.706	0.414
$^{12}_{\Lambda}$C	Exact	0.200	0.628	0.828	0.319
	sWA	0.199	0.594	0.794	0.335
$^{12}_{\Lambda}$C′	Exact	0.205	0.793	0.998	0.259
	sWA	0.201	0.755	0.955	0.266
$^{13}_{\Lambda}$C	Exact	0.241	0.615	0.855	0.391
	sWA	0.238	0.582	0.820	0.409
$^{21}_{\Lambda}$C	Exact	0.340	0.535	0.874	0.635
	sWA	0.335	0.510	0.845	0.657
$^{16}_{\Lambda}$O	Exact	0.253	0.719	0.972	0.352
	sWA	0.250	0.689	0.938	0.362
$^{17}_{\Lambda}$O	Exact	0.279	0.710	0.989	0.393
	sWA	0.275	0.677	0.952	0.406
$^{28}_{\Lambda}$Si	Exact	0.297	0.815	1.112	0.364
	sWA	0.289	0.760	1.049	0.380
$^{29}_{\Lambda}$Si	Exact	0.311	0.806	1.117	0.385
	sWA	0.302	0.751	1.053	0.401

ΛN SRCs are less discussed in the literature. Nevertheless, it was established that the phenomenological spin-independent correlation function in Eq. (21) of Ref. [18], which is the same as that used here, is a good approximation of the full correlation function.

The sWA works very well for any other choice of the OME potential different from the model assumption of $\pi + K$ exchanges considered above. As one example in Table II are also

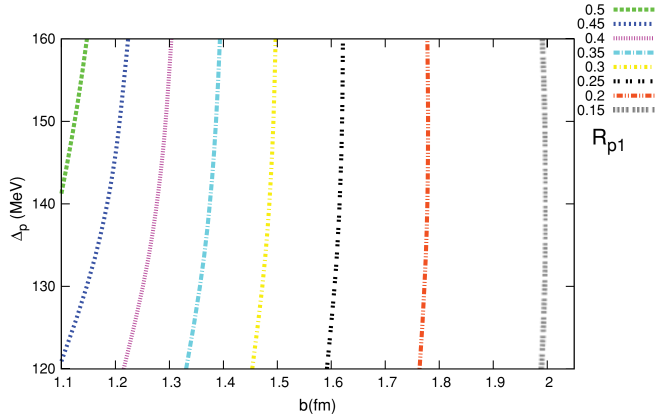

FIG. 1. (Color online) Single-particle decay rate R_{p1} as a function of the length parameter b and the liberated energy Δ_p.

TABLE III. s-shell single-particle decay rates R_{NJ} scaled by a factor of 10. The results for ${}^{9}_{\Lambda}$C and ${}^{9}_{\Lambda}$Be are not shown, since they are the same as those for ${}^{9}_{\Lambda}$He.

${}^{A}_{\Lambda}Z$	$10R_{n0}$	$10R_{n1}$	$10R_{p0}$	$10R_{p1}$
${}^{5}_{\Lambda}$He	0.1411	0.9470	0.0705	2.3620
${}^{7}_{\Lambda}$Li	0.1310	0.8842	0.0655	2.2194
${}^{9}_{\Lambda}$He	0.1228	0.8334	0.0614	2.1026
${}^{11}_{\Lambda}$B	0.1162	0.7915	0.0581	2.0054
${}^{12}_{\Lambda}$C	0.1133	0.7732	0.0567	1.9626
${}^{13}_{\Lambda}$C	0.1107	0.7563	0.0553	1.9230
${}^{21}_{\Lambda}$C	0.0950	0.6557	0.0475	1.6845
${}^{16}_{\Lambda}$O	0.1038	0.7124	0.0519	1.8196
${}^{17}_{\Lambda}$O	0.1018	0.6997	0.0509	1.7894
${}^{28}_{\Lambda}$Si	0.0860	0.5975	0.0430	1.5441
${}^{29}_{\Lambda}$Si	0.0849	0.5905	0.0425	1.5272

shown the results for ${}^{12}_{\Lambda}$C (labelled as ${}^{12}_{\Lambda}$C′) obtained with the full $\pi+\eta+K+\rho+\omega+K^*$ OME potential. It is also evident that more realistic estimates of the oscillator parameter b, as the one given by Itonaga *et al.* [25], would affect both calculations in the same manner, and would yield to the same degree of agreement between the exact and sWA results.[5]

One should keep in mind that in the Fermi gas model, the Λ hyperon is taken to be always in a relative s state with respect to any of the nucleons within the hypernucleus. Therefore, the success of the sWA indirectly justifies the application of such a model to the NMWD of finite nuclei [39].

After fixing the OME potential, all R_{NJ} depend only on b and Δ_N. As an example, the dependence of R_{p1} on these two quantities is illustrated in Fig. 1. The variation of Δ_p has a very small effect, as can be seen from Eq. (2.37). Contrary to this, the R_{NJ} depend very strongly on b through the radial wave function $\mathrm{R}_{00}(\sqrt{2}b, r)$ in Eq. (2.42). The corresponding s-shell single-particle decay rates R_{NJ} are exhibited in Table III. Finally, we note that by using the values listed in Tables I and III, together with Eq. (2.27), we recover the sWA results shown in Table II.

Table III, as well as Fig. 1, clearly show that the size parameter b is the most important nuclear structure parameter for the NMWD rates Γ_n and Γ_p, and therefore the knowledge of its value for each individual hypernuclei could become crucial in comparing the theory with experiments. However, this has not come to pass with the ratio $\Gamma_{n/p}$, which is mainly tailored by the OME potential.

[5]The b values used here of 1.765, 1.781, 1.838, and 1.966 fm for ${}^{11}_{\Lambda}$B, ${}^{12}_{\Lambda}$C, ${}^{16}_{\Lambda}$O, and ${}^{28}_{\Lambda}$Si do not differ much from the values reported in Ref. [25], which are, respectively, 1.65, 1.65, 1.755, and 1.865.

IV. CONCLUSIONS AND SUMMARY

The following conclusions can be drawn regardless of the OME potential that is used:

(i) The sWA is sufficiently accurate for not only for qualitative discussions but also quantitative descriptions of the NMWD in hypernuclei within the IPSM, when the SRCs are described by phenomenological correlation functions as done here.

(ii) The increase of transition rates Γ_n, Γ_p, and Γ_{nm}, as a function of the hypernuclear mass number, stems from the interplay of the increase of $\mathcal{F}_{NJ}$ and the decrease of R_{NJ}.

(iii) The ratio $\Gamma_{n/p}$ is almost the same for all hypernuclei that are on the stability line ($\mathsf{N}=\mathsf{Z}$), i.e., ${}^{5}_{\Lambda}$He, ${}^{7}_{\Lambda}$Li, ${}^{11}_{\Lambda}$B, ${}^{13}_{\Lambda}$C, ${}^{17}_{\Lambda}$O, ${}^{29}_{\Lambda}$Si, etc. Moreover, it decreases when one moves toward the proton drip line ($\mathsf{Z}>\mathsf{N}$) and increases when one goes toward the neutron drip line ($\mathsf{N}>\mathsf{Z}$). It diminishes, for instance, by more than a factor of 4 when going from ${}^{9}_{\Lambda}$He to ${}^{9}_{\Lambda}$C, while the constituent R_{NJ} rates remain the same. It might be somewhat surprising that $\Gamma_n<\Gamma_p$ even when the neutron number is greater than the proton number. But, as seen from Table III, the reason for this is the dominance of $\mathcal{R}_{p1}$ on the other three single-particle decay rates. This dominance, in turn, comes from the dominance of the tensor amplitude d on the remaining amplitudes. The only exception is ${}^{4}_{\Lambda}$H for which $\mathcal{R}_{p1}$ does not contribute.

In summary, using as a tool the IPSM and the s-wave approximation, we have shown that the decay rates Γ_n and Γ_p can be interrelated in a very simple way in all hypernuclei going from ${}^{5}_{\Lambda}$He up to ${}^{29}_{\Lambda}$Si. The relationships between them are particularly simple for the hypernuclei with the same mass number, as illustrated by Eq. (2.41) for the sequence ${}^{9}_{\Lambda}\mathrm{He}\rightarrow{}^{9}_{\Lambda}\mathrm{Be}\rightarrow{}^{9}_{\Lambda}\mathrm{C}$. Results of this type are very likely valid in general, and as such they could be exploited to study experimentally the variations of Γ_n, Γ_p, and $\Gamma_{n/p}$ along many similar arrays in a systematic way.

ACKNOWLEDGMENTS

This work is supported by the Argentinian agency CONICET under Contract PIP 0377. I am grateful to Eduardo Bauer for helpful discussion and critical reading of the manuscript.

[1] C. Samanta, P. Roy Chowdhury, and D. N. Basu, J. Phys. G **35**, 065101 (2008).
[2] A. Sakaguchi *et al.*, arXiv:0904.0298.
[3] E. N. E. van Dalen and A. E. L. Dieperink, Phys. Rev. C **69**, 025802 (2004).
[4] J. Scaffner-Bielich, Nucl. Phys. A **804**, 309 (2008).
[5] J. H. Kim *et al.*, Phys. Rev. C **68**, 065201 (2003).
[6] S. Okada *et al.*, Phys. Lett. B **597**, 249 (2004).
[7] S. Okada *et al.*, Nucl. Phys. A **752**, 196 (2005).
[8] H. Outa *et al.*, Nucl. Phys. A **754**, 157c (2005).
[9] B. H. Kang *et al.*, Phys. Rev. Lett. **96**, 062301 (2006).
[10] M. J. Kim *et al.*, Phys. Lett. B **641**, 28 (2006).

[11] J. D. Parker *et al.*, Phys. Rev. C **76**, 035501 (2007).
[12] H. Bhang *et al.*, Eur. Phys. J. A **33**, 259 (2007).
[13] M. Agnello *et al.*, Nucl. Phys. A **804**, 151 (2008).
[14] M. Agnello *et al.*, Phys. Lett. B **681**, 139 (2009).
[15] M. J. Kim *et al.*, Phys. Rev. Lett. **103**, 182502 (2009).
[16] M. Agnello *et al.*, Phys. Lett. B **685**, 247 (2010).
[17] J. F. Dubach, G. B. Feldman, B. R. Holstein, and L. de la Torre, Ann. Phys. (N.Y.) **249**, 146 (1996).
[18] A. Parreño, A. Ramos, and C. Bennhold, Phys. Rev. C **56**, 339 (1997).
[19] A. Ramos, M. J. Vicente-Vacas, and E. Oset, Phys. Rev. C **55**, 735 (1997); **66**, 039903(E) (2002).
[20] K. Sasaki, T. Inoue, and M. Oka, Nucl. Phys. A **669**, 331 (2000); **678**, 455(E) (2000).
[21] W. M. Alberico and G. Garbarino, Phys. Lett. B **486**, 362 (2000).
[22] J. H. Jun, Phys. Rev. C **63**, 044012 (2001).
[23] K. Sasaki, T. Inoue, and M. Oka, Nucl. Phys. A **707**, 477 (2002).
[24] A. Parreño and A. Ramos, Phys. Rev. C **65**, 015204 (2001).
[25] K. Itonaga, T. Ueda, and T. Motoba, Phys. Rev. C **65**, 034617 (2002).
[26] C. Barbero, D. Horvat, F. Krmpotić, T. T. S. Kuo, Z. Narančić, and D. Tadić, Phys. Rev. C **66**, 055209 (2002).
[27] C. Barbero, C. De Conti, A. P. Galeão, and F. Krmpotić, Nucl. Phys. A **726**, 267 (2003).
[28] F. Krmpotić and D. Tadić, Braz. J. Phys. **33**, 187 (2003).
[29] G. Garbarino, A. Parreño, and A. Ramos, Phys. Rev. Lett. **91**, 112501 (2003).
[30] E. Bauer and F. Krmpotić, Nucl. Phys. A **717**, 217 (2003); **739**, 109 (2004).
[31] A. Parreño, C. Bennhold, and B. R. Holstein, Phys. Rev. C **70**, 051601 (2004).
[32] G. Garbarino, A. Parreño, and A. Ramos, Phys. Rev. C **69**, 054603 (2004).
[33] G. Garbarino, A. Parreño, and A. Ramos, Nucl. Phys. A **754**, 137c (2005).
[34] K. Sasaki, M. Izaki, and M. Oka, Phys. Rev. C **71**, 035502 (2005).
[35] W. M. Alberico, G. Garbarino, A. Parreño, and A. Ramos, Phys. Rev. Lett. **94**, 082501 (2005).
[36] C. Barbero, A. P. Galeão, and F. Krmpotić, Phys. Rev. C **72**, 035210 (2005).
[37] C. Barbero, A. P. Galeão, and F. Krmpotić, Phys. Rev. C **76**, 054321 (2007).
[38] C. Chumillas, G. Garbarino, A. Parreño, and A. Ramos, Phys. Lett. B **657**, 180 (2007).
[39] E. Bauer, Nucl. Phys. A **781**, 424 (2007); **796**, 11 (2007).
[40] K. Itonaga, T. Motoba, T. Ueda, and Th. A. Rijken, Phys. Rev. C **77**, 044605 (2008).
[41] C. Barbero, A. P. Galeão, M. S. Hussein, and F. Krmpotić, Phys. Rev. C **78**, 044312 (2008); **78**, 059901(E) (2008).
[42] E. Bauer, A. P. Galeão, M. Hussein, F. Krmpotić, and J. D. Parker, Phys. Lett. B **674**, 103 (2009).
[43] E. Bauer and G. Garbarino, Nucl. Phys. A **828**, 29 (2009).
[44] E. Bauer, Nucl. Phys. A **818**, 174 (2009).
[45] E. Bauer and G. Garbarino, Phys. Rev. C **81**, 064315 (2010).
[46] E. Bauer, A. P. Galeão, M. S. Hussein, and F. Krmpotić, Nucl. Phys. A **834**, 599c (2010).
[47] E. Bauer and G. Garbarino, Nucl. Phys. A **835**, 430 (2010).
[48] E. Bauer, G. Garbarino, A. Parreño, and A. Ramos, Nucl. Phys. A **836**, 199 (2010).
[49] F. Conti, A. Meucci, C. Giusti, and F. D. Pacati, arXiv:0912.3630.
[50] W. M. Alberico and G. Garbarino, Phys. Rep. **369**, 1 (2002) ; in *Hadron Physics, Proceedings of the International School of Physics Enrico Fermi, Course CLVIII, Varenna, Italy*, edited by T. Bressani, A. Filippi and U. Wiedner (IOS Press, Amsterdam, 2005), p. 125.
[51] H. Outa, in *Hadron Physics, Proceedings of the International School of Physics Enrico Fermi, Course CLVIII, Varenna, Italy*, edited by T. Bressani, A. Filippi and U. Wiedner (IOS Press, Amsterdam, 2005), p. 219.
[52] A. Parreño, Lect. Notes Phys. **724**, 141 (2007).
[53] C. Chumillas, G. Garbarino, A. Parreño, and A. Ramos, Nucl. Phys. A **804**, 162 (2008).
[54] M. M. Block and R. H. Dalitz, Phys. Rev. Lett. **11**, 96 (1963).
[55] J. Cohen, Prog. Part. Nucl. Phys. **25**, 139 (1990).
[56] J. Ryckebusch, M. Vanderhaeghen, L. Machenil, and M. Waroquier, Nucl. Phys. A **568**, 828 (1994).
[57] A. P. Galeão, AIP Conf. Proc. **739**, 560 (2004).
[58] M. Moshinsky, Nucl. Phys. **13**, 104 (1959).
[59] I. S. Gradshteyn and I. M. Ryzhnik, *Tables of Integrals, Series, and Products* (Academic, New York, 1965).
[60] A. Bohr and B. R. Mottelson, *Nuclear Structure* (Benjamin, New York, 1969), Vol. I.